PROCEEDINGS OF SCIENCE

Study of the process $e^+e^- \to K^+K^-\pi^+\pi^-$ in the c.m. energy range 1.5 - 2.0 GeV with the CMD-3 detector

R.R.Akhmetshin[a], A.V.Anisenkov[a], V.M.Aulchenko[ab], V.S.Banzarov[a], N.S.Bashtovoy[a], D.E.Berkaev[ab], A.V.Bragin[a], S.I.Eidelman[ab], D.A.Epifanov[af], L.B.Epshteyn[ac], A.L.Erofeev[a], G.V.Fedotovich[ab], S.E.Gayazov[ab], A.A.Grebenuk[ab], D.N.Grigoriev[abc], E.M.Gromov[a], F.V.Ignatov[a], S.V.Karpov[a], V.F.Kazanin[ab], B.I.Khazin[ab], A.N.Kirpotin[a], I.A.Koop[ab], O.A.Kovalenko[ab], A.N.Kozyrev[a], E.A.Kozyrev[ab], P.P.Krokovny[ab], A.E.Kuzmenko[ac], A.S.Kuzmin[a], I.B.Logashenko[ab], P.A.Lukin[ab], A.P.Lysenko[a], K.Yu.Mikhailov[ab], V.S.Okhapkin[a], Yu.N.Pestov[a], E.A.Perevedentsev[ab], A.S.Popov[ab], Yu.S.Popov[a], G.P.Razuvaev[ab], Yu.A.Rogovsky[a], A.L.Romanov[a], A.A.Ruban[a], N.M.Ryskulov[a], A.E.Ryzhenenkov[ab], V.E.Shebalin[a], D.N.Shemyakin*[ab], B.A.Shwartz[ab], D.B.Shwartz[ab], A.L.Sibidanov[ad], P.Yu.Shatunov[a], Yu.M.Shatunov[a], E.P.Solodov[ab], V.M.Titov[a], A.A.Talyshev[ab], A.I.Vorobiov[a], Yu.V.Yudin[a], Yu.M.Zharinov[a]

[a] *Budker Institute of Nuclear Physics, SB RAS, Novosibirsk, 630090, Russia*
[b] *Novosibirsk State University, Novosibirsk, 630090, Russia*
[c] *Novosibirsk State Technical University, Novosibirsk, 630092, Russia*
[d] *University of Sydney, Falkiner High Energy Physics, NSW 2006, Sydney, Australia*
[f] *University of Tokyo, Department of Physics, 7-3-1 Hongo Bunkyo-ku Tokyo, 113-0033, Japan*
E-mail: dimnsh@yandex.ru

We report preliminary results on the measurement of the $e^+e^- \to K^+K^-\pi^+\pi^-$ cross section in the c. m. energy range from 1.5 GeV to 2 GeV. It was found that the cross section is dominated by the contributions of the $K^+K^-\rho$, $K^*K\pi$, $\phi\pi^+\pi^-$ and K^*K^* intermediate states.

Keywords : e^+e^- colliders, hadrons, detectors.

XV International Conference on Hadron Spectroscopy-Hadron 2013
4-8 November 2013
Nara, Japan

*Speaker.

PoS(Hadron 2013)138

1. Introduction

The process $e^+e^- \to K^+K^-\pi^+\pi^-$ has been studied at DM1 [1], DM2 [2] and with much larger effective integrated luminosity at the BaBar by ISR [3, 4]. Study of production dynamics with BaBar exhibited complex resonant substructures ($K^+K^-\rho$, $K^*K\pi$, $\phi\pi^+\pi^-$, K_1K etc.). Part of $e^+e^- \to K^+K^-\pi^+\pi^-$ intermediate states were studied by the Babar collaboration, but it is possible to make a more detailed analysis of this dynamics with the CMD-3 detector [5].

Precise data on the cross sections of $e^+e^- \to$ hadrons are also required to evaluate the muon anomalous magnetic moment $a_\mu = (g-2)_\mu/2$. In the case of $a_\mu^{\rm had}$, the VEPP-2000 energy range gives the major contribution ($\sim 92\%$) both to the value of the hadronic vacuum polarization itself and to its uncertainty. Using isospin relations, based on value of the $e^+e^- \to K^+K^-\pi^+\pi^-$ cross section the contributions from various $K\bar{K}\pi\pi$ final states in the energy range up to 2 GeV are estimated to be $(3.31 \pm 0.58) \times 10^{-10}$ [6]. So the independent measurements of the $e^+e^- \to K^+K^-\pi^+\pi^-$ cross section with high precision are very important.

The presented result on the $e^+e^- \to K^+K^-\pi^+\pi^-$ cross section is based on 22 pb^{-1} of data collected with the CMD-3 detector at the VEPP-2000 collider [7] in the c.m. energy range from 1.5 to 2.0 GeV. The luminosity is measured using events of Bhabha scattering at large angles [8].

An important feature of this analysis is two independent approaches for event selection. The first one, based on the difference between pion and kaon ionization losses in the Drift Chamber [9], will be discussed in the second section. The second, based on the energy-momentum conservation, will be described in the third section.

2. $K\pi$ separation

As one can see from Fig. 1, the ionization losses of pions and kaons in the Drift Chamber are significantly different. Therefore K π separation is based on the analysis of the likelihood function using information about ionization losses (dE/dx) in DC. The probability density function

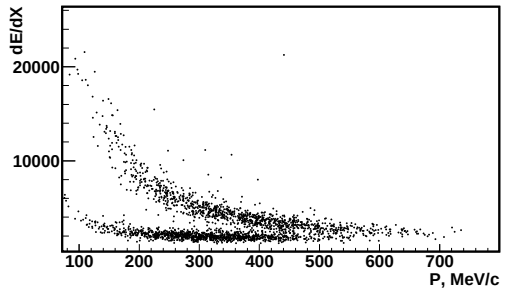

Figure 1: Pion and kaon ionization losses in DC vs particle momentum.

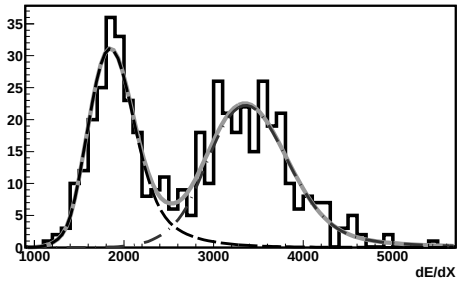

Figure 2: PDF of pion and kaon ionization losses in DC for the momentum interval from 400 to 450 MeV/c.

(PDF) with momentum and dE/dx as arguments is constructed for kaons f_K(p,dE/dx) and pions f_π(p,dE/dx):

$$f_{K,\pi}(\mathrm{p},\mathrm{dE/dx}) = \mathrm{N}_G \times G(<\mathrm{dE/dx}>,\sigma_G) + \mathrm{N}_{Gl} \times Gl(<\mathrm{dE/dx}>,\sigma_{Gl},\eta).$$

where $G(< dE/dx >, \sigma_G)$ is the Gaussian function, $Gl(< dE/dx >, \sigma_{Gl}, \eta)$ is the logarithmic Gaussian function. The latter is necessary to describe the tails of the distribution of the ionization losses. The average ionization losses <dE/dx>, standard deviations σ_G and σ_{Gl}, asymmetry η, amplitudes N_{Gl} and N_G depend only on a momentum. The PDF parameters are determined by approximation of the dE/dx vs momentum histogram. First of all f_π(p,dE/dx) is determined using a sample of test $e^+e^- \to \pi^+\pi^-\pi^+\pi^-$ events, then f_K(p,dE/dx) function is determined using a sample of test $e^+e^- \to K^+K^-\pi^+\pi^-$ events with fixed f_π(p,dE/dx). This procedure was performed for simulated and experimental data at each energy point. The example of PDF is shown in Fig. 2 as a smooth curve line for momenta 400 - 450 MeV/c.

The likelihood function ($L_{KK\pi\pi}$) is defined as:

$$L_{KK\pi\pi} = Log\Big(\frac{\prod_i f^i_{\alpha_i}(p, dE/dx)}{\prod_i [f^i_\pi(p, dE/dx) + f^i_K(p, dE/dx)]}\Big),$$

where i - track index, α_i - supposed type (K or π) of particle, which is produced by the i-track. The $L_{KK\pi\pi}$ is constructed for events with three or four tracks in the Drift Chamber, so track index changes from 1 to 3 or 4, respectively. $L_{KK\pi\pi}$ is constructed under the assumption that each event is a $K^+K^-\pi^+\pi^-$ event, so two tracks should be identified as kaons and other two as pions. Therefore, taking into account all the permutations and charges of the particles, $L_{KK\pi\pi}$ receives four different values for each event. The most probable combination of particle types provides a maximum of this function. The distribution of such defined maximum values of $L_{KK\pi\pi}$ for experimental data shown in Fig. 3. The open histogram corresponds to all four-track events while the hatched one and shaded to $\pi^+\pi^-\pi^+\pi^-$ and $K^+K^-\pi^+\pi^-$ events respectively. It is seen that the likelihood function value is a good parameter to select $e^+e^- \to K^+K^-\pi^+\pi^-$ events from background. The condition for the $L_{KK\pi\pi}$ value to be larger than -2 was chosen as a mild condition, which allows to suppress background by a factor of 20 and preserve more than 99% of useful events.

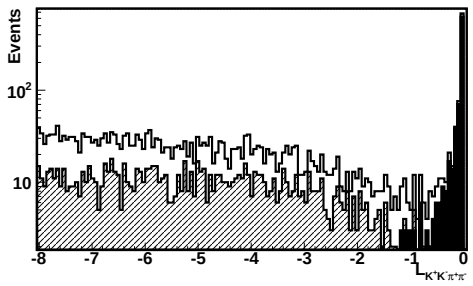

Figure 3: Distribution of the maximum likelihood function ($L_{KK\pi\pi}$) value for the four-track events. The open histogram corresponds to all four-track events, the hatched one does $\pi^+\pi^-\pi^+\pi^-$ events and the shaded one - $K^+K^-\pi^+\pi^-$ events.

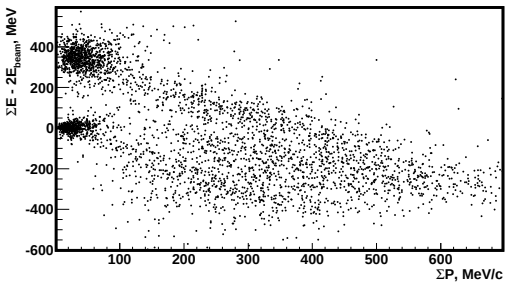

Figure 4: Scatter plot of the difference between the total energy and c.m. energy (ΔE_4) versus the total momentum for four-track events. The upper cluster of dots represents $\pi^+\pi^-\pi^+\pi^-$ while the lower one - $K^+K^-\pi^+\pi^-$ events.

3. Selection of $e^+e^- \to K^+K^-\pi^+\pi^-$ events

Candidates for the process under study are required to have in the Drift Chamber three or four tracks coming from the interaction region. Momentum of charged particle $\vec{p}_i$ is defined according

to the track curvature and angles reconstructed in DC. After the types of particles in three- or four-track events were defined using method described above, the total energy E_{tot} and total momentum P_{tot} could be used for selection of four-track $e^+e^- \to K^+K^-\pi^+\pi^-$ events. They are defined as:

$$\mathrm{E_{tot}} = \sum_{\mathrm{i}=1}^{4} \sqrt{\mathrm{p_i^2} + \mathrm{m_i^2}}, \mathrm{P_{tot}} = |\sum_{\mathrm{i}=1}^{4} \vec{\mathrm{p}}_\mathrm{i}|.$$

Figure 4 shows a scatter plot of the difference between the measured total energy and c.m. energy $\Delta E_4 = E_{tot} - E_{c.m.}$ vs the total momentum for events with four tracks. The condition for $L_{KK\pi\pi}$ is not used for events on this histogram. The signal events locate near zero on the vertical axis and near zero on the horisontal axis. The another cluster of events with a zero total momentum but shifted up the vertical axis, corresponds to $\pi^+\pi^-\pi^+\pi^-$ events. The conditions on ΔE_4 and P_{tot} for the signal events were chosen as:

$$-100\,\mathrm{MeV} < \Delta\mathrm{E_4} < 100\,\mathrm{MeV},\ \mathrm{P_{tot}} < 100\,\mathrm{MeV}/c.$$

Energy deficit should correlate with the total (missing) momentum for the three-track candidates. The track loss can be caused by the DC reconstruction inefficiency or limited DC acceptance. Using the total momentum of three-track candidates, the energy of a missing particle was calculated and added to the energy of three detected particles. The difference between the obtained energy ΔE_{3+1} and c.m. energy is shown in Fig. 5. Here the condition on the $L_{KK\pi\pi}$ is applied. A signal events are clearly seen near zero. To obtain the number of $K^+K^-\pi^+\pi^-$ events from a three-track sample, the histogram was fitted with a sum of two Gaussian distributions for a signal peak and a quadratic polynomial for background in range from -200 MeV to 200 MeV. Variation of fitting functions for the peak and background leads to about 3% uncertainty in the number of signal events.

As a result, $\sim$13300 four-track events and $\sim$16000 three-track events were selected. To obtain a detection efficiency, the $K^+K^-\pi^+\pi^-$ events were simulated with a primary generator using the GEANT4 package and then reconstructed with the same software as experimental data. Production mechanisms with the $K^+K^-\rho$, $K_1K \to K^*\pi K$, $\phi\pi^+\pi^-$ and K^*K^* interfering intermediate states are used for the primary generator to describe angular and invariant mass distributions of the experimental data. The total detection efficiency takes into account the contributions of different intermediate states based on the approximation of the experimental angular and momentum distributions. A phase space model was also considered and excluded from further consideration because it contradicted to all studied distributions.

4. Cross section calculation and Summary

At each energy point the cross section is calculated as

$$\sigma = \frac{N_{4\mathrm{tr}} + N_{3\mathrm{tr}}}{L \cdot \varepsilon \cdot (1+\delta)},$$

where L is the integrated luminosity, ε is the detection efficiency, and $(1+\delta)$ is the radiative correction calculated according to [10, 11]. The detection efficiency is about 50-60 % and is basically determined by detector acceptance. The radiative correction smoothly increases from 0.8

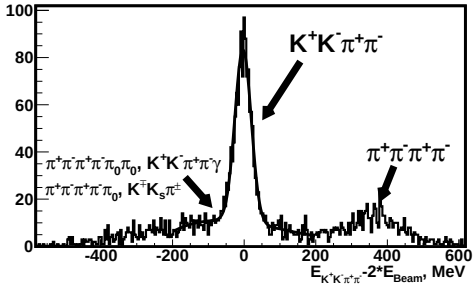

Figure 5: The histogram of the difference between the calculated energy of the fourth particle ΔE_{3+1} and c.m. energy.

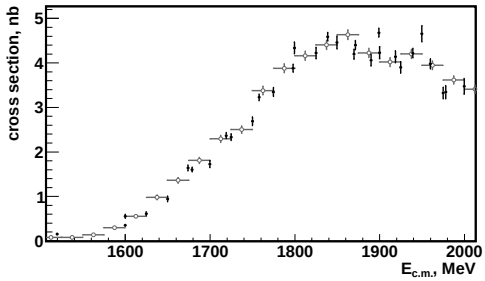

Figure 6: Dots show the ee $e^+e^- \to K^+K^-\pi^+\pi^-$ cross section measured with the CMD-3 detector. The BaBar results are shown by open circles.

to 0.98 in the studied energy range. The cross section as a function of energy is presented in Fig. 6. The cross section maximum value is ~ 4.5 nb. Systematic errors are under study and are currently estimated as 7%. The main uncertainty is due to model dependence of the detection efficiency. The obtained cross section agrees with the previous measurement by the BaBar Collaboration [4] presented by open circles.

5. Acknowledgments

The authors are grateful to A.I. Milstein for many useful discussions.

This work is supported in part by the Ministry of Education and Science of the Russian Federation, by FEDERAL TARGET PROGRAM "Scientific and scientific-pedagogical personnel of innovative Russia in 2009-2013", by agreement 14.B37.21.07777, by the RFBR grants 10-02-00253, 10-02-00695, 11-02-00112, 11-02-00328, 12-02-01032, 12-02-31498, 12-02-31499, 12-02-31501, 13-02-00215, 14-02-00047 and the DFG grant HA 1457/9-1.

References

[1] A. Cordier *et al.*, Phys. Lett. **B110**, 335 (1982).

[2] D. Bisello *et al.*, Nucl.Phys.Proc.Suppl. **21**, 111 (1991).
M.R. Whalley, J. Phys. **G29**, A1 (2003).

[3] B. Aubert *et al.*, Phys. Rev. **D77**, 092002 (2008).

[4] J.P. Lees *et al.*, Phys. Rev. **D86**, 012008 (2012).

[5] B.I. Khazin *et al.*, Nucl. Phys. B (Proc. Suppl.) **181-182**, 376 (2008).

[6] K. Hagiwara *et al.*, J. Phys. **G38**, 085003 (2011).

[7] D.E. Berkaev *et al.*, JETP **113**, 213 (2011).

[8] R.R. Akhmetshin *et al.*, Nucl. Phys. B (Proc. Suppl.) **225-227**, 69 (2012).

[9] F. Grancagnolo *et al.*, Nucl. Instr. Meth. A**623**, 114 (2010).

[10] E.A. Kuraev and V.S. Fadin, Sov. J. Nucl. Phys. **41**, 466 (1985).

[11] S. Actis *et al.*, Eur. Phys. J. **C66**, 585 (2010).